A systematic study of water models for molecular simulation: Derivation of water models optimized for use with a reaction field

David van der Spoel,[a] Paul J. van Maaren, and Herman J. C. Berendsen[b]
Bioson Research Institute and Laboratory of Biophysical Chemistry, University of Groningen, Nijenborgh 4, 9747 AG Groningen, The Netherlands

(Received 22 July 1997; accepted 29 January 1998)

We have performed long molecular dynamics simulations of water using four popular water models, namely simple point charge (SPC), extended simple point charge (SPC/E), and the three point (TIP3P) and four point (TIP4P) transferable intermolecular potentials. System sizes of 216 and 820 molecules were used to study the dependence of properties on the system size. All systems were simulated at 300 K with and without reaction fields and with two different cutoff radii, in order to study the impact of the cutoff treatment on density, energy, dynamic, and dielectric properties. Furthermore we generated two special-purpose water models based on the SPC and TIP4P models, for use with a reaction field. The atomic charges and the Lennard-Jones C_{12} parameter were optimized to reproduce the correct energy and pressure using the weak coupling algorithm for parameters. Indeed, in simulations without parameter coupling of both new models the density and potential energy were found to be close to the experimental values. The other properties of these models that we called SPC/RF and TIP4P/RF (where RF stands for reaction field) are evaluated and discussed. © *1998 American Institute of Physics.* [S0021-9606(98)51317-7]

I. INTRODUCTION

It is well-known that the use of cutoffs for nonbonded interactions in molecular simulations has many undesired effects. For Lennard-Jones interactions there is a small energetic effect, but a large effect on the pressure. For homogeneous systems these effects can be corrected analytically.[1] When pressure scaling is applied, the pressure correction should in principle be done during the simulation, because the correction is usually in the order of several hundred bar.

When dipolar electrostatic interactions are present in the simulation system, the situation becomes worse. In the case of water a number of popular models, such as SPC,[2] TIP3P, and TIP4P (Ref. 3) and SPC/E (Ref. 4) are often simulated with a cutoff of about 1.0 nm. This is justified in part by the experimental radial distribution functions[5,6] which do not show any features after 0.9 nm. However, the absence of such features does not mean there is no liquid structure beyond this distance. Computer simulations have shown considerable ordering in water up to a molecular separation of about 1.4 nm.[7] By plotting the distance-dependent finite system Kirkwood factor G_k (Ref. 8) a significant dip in the curve at the cutoff becomes apparent. The implication of this effect is that the dielectric properties of the simulated water are not treated appropriately. A related problem caused by cutoffs for electrostatic interactions is that when a molecule leaves the cutoff range of another molecule, there is still some orientational correlation between the two molecules, but since there is no interaction at all beyond the cutoff, a molecule entering the cut-off range of another molecule will in principle not be appropriately correlated.[9] This effect adds noise to the simulation system and therefore causes considerable heating. When no temperature scaling is applied, the system will warm up within 10 ps, and the total energy is not conserved.

The largest problem with cutoffs is encountered when full charges are present in the simulation system. In such a case accumulation of charge at the cutoff distance occurs.[10,11] When two equally charged ionic groups are within the cutoff they will repel each other until the distance is greater than the cutoff. After that the ionic groups will diffuse randomly until they approach each other to within the cutoff distance. This effect can be clearly shown by plotting radial distribution functions.[10–12] It should be stressed that this effect is important for simulations of salt solutions as well as of biological macromolecules, such as proteins, DNA, and phospholipids.

A number of methods exist for the explicit treatment of long-range electrostatic interactions, the most prominent being the Ewald summation method,[1,13] others are particle–particle particle–mesh (PPPM) (Refs. 14, 15) or particle–mesh Ewald (PME) (Refs. 16, 17) methods and hierarchical methods.[18] It is however not the aim of this paper to discuss these methods in full. Rather, we want to focus on another well-known method to treat electrostatic interactions, the reaction field approach.[8,19–23] This method, which is applicable to homogeneous systems only, assumes a dielectric continuum beyond a given cutoff radius r_c with a dielectric constant of $\varepsilon_{\mathrm{rf}}$. The net effect of this dielectric environment is that all interactions are screened, and the force at the cutoff distance is nearly zero. The ''classical'' reaction field method can be used for polar liquids only when no ionic groups are present. This approach was extended by Tironi

[a]Present address: Department of Biochemistry, University of Uppsala, Husargatan 3, Box 576, 751 23 Uppsala, Sweden.
[b]Corresponding author.

et al. to include a contribution from ions in the solution, by assuming a dielectric continuum with a given ionic strength beyond the cutoff r_c.[24] Under the constraint that the entire simulation system is electroneutral, the generalized reaction field method as the authors named it, yields a simple force formula that in the limit of zero ionic strength reduces to the classical reaction field. A number of other methods to smooth electrostatic interactions to zero at the cutoff distance are in practical use, but since these methods are not based on a clear physical idea, they should be regarded as part of the force field parameterization. Moreover, such ad hoc smoothing functions have been shown to disturb the dipole–dipole correlation, leading to unrealistic dielectric behavior.[25]

One of the major drawbacks of adding a reaction field term to the potential, or of using a long-range electrostatics method is that the force fields in use today were, to our knowledge, all developed without such terms, and the parameters in the model may be expected to depend on the method used to parameterize them. In simulations of water with a reaction field the density was found to be lower than the experimental value, and the potential energy higher.[26] In free energy calculations using a reaction field it was found that the free energy of hydration of acetamide was -7.4 kcal/mol, while without the reaction field it was -9.2 kcal/mol, the experimental value being -9.7 kcal/mol.[7] It should be noted however, that this is an ''extreme'' example, because acetamide has a large dipole. With such discrepancies in mind it seems reasonable to be reluctant in the application of methods like the reaction field, because considerable reparameterization of force fields will be necessary before the ''accuracy'' of the existing force field is regained.[27]

In this work, we present 1.0 ns simulations of a reasonably sized water system (820 molecules) using different water models [SPC,[2] SPC/E,[4] TIP3P, and TIP4P (Ref. 3)] with and without reaction field and with cutoffs of 0.9 nm and 1.2 nm. To test the effects of system size we have also simulated smaller boxes of 216 molecules for each of the water models with a cutoff of 0.9 nm and with and without reaction field. Our first aim is to quantify the dependence of density and energy, and dynamic and dielectric properties on cutoff length, system size and use of the reaction field. For consistency we used the reaction field method together with long-range corrections for Lennard-Jones interactions.[1] It may seem excessive to perform all these simulations when most of the data can be found in the scientific literature. However, we felt it necessary to perform all simulations under exactly the same conditions and using the same system sizes. We also wished to calculate all relevant properties from the simulations with the same method. Finally, with this set of simulations of different water models, it is possible to get a good insight into the influence of the simulation methodology (cutoff, system size, reaction field) on the results.

Our second goal was to reparameterize both SPC and TIP4P for use with a reaction field. A number of authors have suggested that with the use of a reaction field the force field has to be reparameterized[7,24] which is what we have set out to do here. We again apply long-range corrections for Lennard-Jones interactions, in the hope that our new Lennard-Jones parameters will not depend on the cutoff. For this purpose, the weak-coupling scheme for force field parameterization was used.[28,29] This method has been tested on a number of systems, like water,[28,30] liquid mercury[29] and polarizable water.[31] We have implemented the method in the GROMACS molecular dynamics package,[32,33] in a quite general way, to facilitate force field optimization for charges and Lennard-Jones parameters of any model system.

II. THEORY

The contribution of a pair i,j to the potential energy and the forces in the presence of a reaction field are[8]

$$V_{\mathrm{crf}} = f\frac{q_i q_j}{r_{ij}}\left[1+\frac{\varepsilon_{\mathrm{rf}}-1}{2\varepsilon_{\mathrm{rf}}+1}\frac{r_{ij}^3}{r_c^3}\right], \tag{1}$$

$$\boldsymbol{F}_i(\mathbf{r}_{ij}) = f q_i q_j\left[\frac{1}{r_{ij}^3}-\frac{\varepsilon_{\mathrm{rf}}-1}{2\varepsilon_{\mathrm{rf}}+1}\frac{2}{r_c^3}\right]\mathbf{r}_{ij} \quad (r_{ij}<r_c), \tag{2}$$

where $f=(1/4\pi\epsilon_0)$, q_i and q_j are the atomic charges of atoms i and j, respectively, r_c is the cutoff, and $\varepsilon_{\mathrm{rf}}$ is the dielectric permittivity of the continuum.

We have applied long-range corrections for the dispersion interaction[1] according to

$$V_{lr} = -\tfrac{2}{3}N\rho\pi C_6 r_c^{-3}, \tag{3}$$

$$P_{lr} = -\tfrac{4}{3}\pi C_6 \rho^2 r_c^{-3}, \tag{4}$$

where C_6 is the force constant, ρ is the number density of Lennard-Jones particles, which in the case of the water models are only the oxygen atoms, and N is the number of Lennard-Jones particles.

We use the general coupling theory (GCT) (Ref. 28) or parameter coupling[29,30] to modify our force field during the simulation. The method is rather simple; it is based on the weak coupling algorithm for temperature and pressure control in molecular dynamic (MD) simulations.[34] In this method the force field parameters are modified during the simulation, in such a way that an observable of the simulation, for example the potential energy relaxes slowly towards a given reference value. We have implemented modification of Lennard-Jones C_{12} and C_6 and of charges, which can either be coupled to the total potential energy or to the total pressure. Extension to other observables is straightforward. The equation for the case of coupling of a charge q to the energy E is

$$q(t+\Delta t) = q(t)\left[1+\frac{\Delta t}{\xi_E}(E_{\mathrm{ref}}-E)\right], \tag{5}$$

where Δt is the integration time step, and ξ_E is a user-supplied parameter which has the dimension of time$\times$energy, and E_{ref} is the target energy. The size of ξ determines the time constant τ_E of the coupling. Equation (5) implies that

$$\frac{\mathrm{d}q}{\mathrm{d}t} = \frac{E_{\mathrm{ref}}-E}{\xi_E} \approx \frac{q_{\mathrm{ref}}-q}{\tau_E}, \tag{6}$$

TABLE I. Force field parameters and electrostatic properties of the water models used.

Model	qO (e)	qH (e)	$C6$ (kJ mol^{-1} nm^6)	$C12$ (kJ mol^{-1} nm^{12})	Dipole (Debye)
SPC	−0.82	0.41	2.6171e-3	2.6331e-6	2.27
SPC/E	−0.8476	0.4238	2.6171e-3	2.6331e-6	2.39
TIP3P	−0.834	0.417	2.4889e-3	2.4352e-6	2.35
TIP4P	−1.04	0.52	2.5543e-3	2.5145e-6	2.18
SPC/RF	−0.8124	0.4062	2.6171e-3	2.4768e-6	2.25
TIP4P/RF	−1.0426	0.5213	2.5543e-3	2.45e-6	2.18

where

$$\tau_E = \xi_E \left\langle \frac{\partial E}{\partial q} \right\rangle^{-1}. \tag{7}$$

Hence the parameter q is expected to converge smoothly to its correct reference value by a first order process with a time constant τ_E. The dependence of observables on parameters have been determined by Berendsen *et al.* They derived a value for $\langle \partial E/\partial q_H \rangle$ of -260 kJ mol^{-1} e^{-1}.[4] Zhu and Wong have performed extensive sensitivity analyses of water thermodynamics.[35] They reported a higher value of -50 kJ mol^{-1} e^{-1} for $\langle \partial E/\partial q_H \rangle$. In a similar fashion derivatives of observables with respect to other force field parameters were derived by Berendsen *et al.* (a.o. $\langle \partial P/\partial C_{12} \rangle$) and many more by Zhu and Wong. The latter authors also performed sensitivity analyses for the dependence of distribution functions (a.o. radial distribution functions) on parameters.[36] Use of this information may speed up force field parameterization considerably.

The coupling of force field to parameters should be weak, the time constant τ_E should be about 10 ps, otherwise the algorithm may become unstable. Thus we should apply a ξ_E of about -10^6. Note that the exact value of ξ_E is not important, but its sign is (see Table I).

It is advantageous to apply GCT to two variables simultaneously. Although matrix coupling in the proper gradient direction is possible, we found that good results are obtained (fast convergence) when each parameter is coupled to a distinct observable, and therefore we applied the method in this simple fashion.

III. METHODS

Two cubic boxes, the first with an edge of 3.0 nm, the second with an edge of 1.86 nm, were filled with water molecules of either SPC, SPC/E, TIP3P or TIP4P models. The larger box contained 820 molecules, the smaller 216. With each of the large boxes simulations were performed with cutoff r_c of either 0.9 or 1.2 nm; with the small boxes only a cutoff of 0.9 nm could be used. All simulations were performed with and without a reaction field with $\varepsilon_{\mathrm{rf}} = 78.5$. In the simulations with a reaction field long range corrections for dispersion were applied [Eqs. (3), (4)]. All other parameters were the same in the simulations; temperature scaling was applied using the weak coupling scheme[34] to a bath of 300 K using a time constant of 100 fs, pressure scaling was applied with a reference pressure of 1 bar, and a time constant of 1 ps. The SETTLE algorithm was used to constrain bond length and bond angles,[37] allowing an integration time step of 2 fs. Neighbor lists were used and updated every 20 fs. Neighbor searching was done based on molecules; when the distance between the centers of geometry of two molecules was less than the cutoff, then that molecule pair was taken into account in the simulation.[38] Coordinates were saved every 500 fs, energies were saved every 100 fs. The simulations were 500 000 steps, or 1.0 ns long.

The GCT simulations were performed starting from the 820 molecule boxes of SPC and TIP4P. The charges were coupled to the potential energy with coupling constant $\xi_E = -10^6$, the target value being -41.7 kJ mol^{-1}.[39] The Lennard-Jones C_{12} was coupled to the pressure with coupling constant $\xi_P = 10^6$, the target value was 1 bar. For both systems two 500 ps simulations were performed at constant volume and experimental density. Long range corrections for energy and pressure due to dispersion interactions were used in the parameterization. The starting parameters for the simulations were taken on purpose to be somewhat off the original parameterization to be able to check whether the two runs converge.

The resulting parameter sets for the two models that we named SPC/RF and TIP4P/RF, respectively, were used to perform three simulations each (see Table I). The conditions were exactly the same as with reference simulations described above, 216 molecules with reaction field, and $r_c = 0.9$ nm, and 820 molecules with reaction field and $r_c = 0.9$ nm and 1.2 nm.

In total 24 reference simulations were performed, 4 GCT simulations, and 6 simulations for testing the new water models. All simulations were performed with the GROMACS molecular dynamics and trajectory analysis package[32,33] on SGI computers with MIPS R10k processors. Run times were 11 h for the SPC ($r_c = 0.9$ nm), 24 h for SPC ($r_c = 1.2$ nm), 24 h for TIP4P ($r_c = 0.9$ nm), respectively, 32 h for TIP4P ($r_c = 1.2$ nm).

IV. RESULTS AND DISCUSSION

From the 1.0 ns simulations the first 100 ps were regarded as equilibration, leaving 900 ps for analysis purposes. Thermodynamic properties (density, potential energy, temperature, and pressure) and dielectric properties [finite system Kirkwood factor G_k, infinite system Kirkwood factor g_k, dielectric constant $\varepsilon(0)$, dielectric relaxation time of the system τ_M, and Debye relaxation time τ_D] are given in Table II. The finite system Kirkwood factor G_k can be determined from

$$G_k = \frac{\langle \boldsymbol{M}^2 \rangle}{N \langle \mu^2 \rangle}, \tag{8}$$

where $\boldsymbol{M}$ is the dipole moment of the total simulation system, N is the number of molecules, and μ is the dipole of a single molecule. The infinite system Kirkwood factor g_k is related to the finite system Kirkwood factor G_k by[40]

$$g_k = \frac{(2\varepsilon_{\mathrm{rf}} + \varepsilon(0))(2\varepsilon(0)+1)}{3\varepsilon(0)(2\varepsilon_{\mathrm{rf}}+1)} G_k. \tag{9}$$

TABLE II. Overview of properties from the reference simulations and the simulations with the new SPC/RF and TIP4P/RF water models, derived from the last 900 ps. Averages and rms fluctuations (in parentheses) for density ρ, potential energy E_{pot}, temperature T, and pressure P, finite- and infinite system Kirkwood G factors (G_k and g_k) and dielectric constant $\varepsilon(0)$ are given. The error estimates for $\varepsilon(0)$, A, τ_M, $\varepsilon(\infty)$, and τ_D are, 5 (see text), 0.01, 0.1 ps, 0.5, and 0.1 ps, respectively. Long range dispersion corrections are included in E_{pot} and P for all simulations where $\varepsilon_{\mathrm{rf}}>1$.

Model	N	r_c (nm)	$\varepsilon_{\mathrm{rf}}$	ρ (kg/ℓ)	E_{pot} (kJ/mol)	T (K)	P (bar)	G_k	g_k	$\varepsilon(0)$	A	τ_M (ps)	$\varepsilon(\infty)$	τ_D (ps)
SPC	216	0.9	1.0	0.976(10)	−41.6(0.33)	302 (8.7)	1 (620)							
			78.5	0.967(10)	−41.0(0.33)	303 (8.7)	1 (630)	2.59	2.39	61	0.918	3.5	4.6	4.7
	820	0.9	1.0	0.975 (5)	−41.7(0.18)	303 (4.5)	1 (320)							
			78.5	0.968 (6)	−41.0(0.17)	304 (4.4)	1 (320)	2.70	2.55	65	0.874	3.8	6.9	5.1
		1.2	1.0	0.988 (4)	−42.2(0.16)	301 (4.4)	1 (330)							
			78.5	0.971 (5)	−41.3(0.16)	301 (4.4)	1 (320)	2.64	2.47	63	0.869	4.1	7.1	5.5
SPC/E	216	0.9	1.0	1.001(11)	−46.8(0.37)[a]	302 (8.8)	1 (670)							
			78.5	0.992(13)	−46.0(0.35)	303 (8.8)	1 (660)	2.63	2.53	69	0.928	4.6	4.5	6.4
	820	0.9	1.0	1.001 (6)	−46.9(0.19)	303 (4.5)	1 (340)							
			78.5	0.995 (5)	−46.0(0.18)	303 (4.5)	1 (340)	2.68	2.60	72	0.940	4.8	4.0	6.9
		1.2	1.0	1.008 (6)	−47.2(0.18)	301 (4.4)	1 (340)							
			78.5	0.997 (6)	−46.4(0.18)	301 (4.4)	1 (340)	2.89	2.93	81	0.922	6.6	5.2	9.7
TIP3P	216	0.9	1.0	0.989(10)	−40.2(0.31)	303 (8.6)	1 (620)							
			78.5	0.972(11)	−39.3(0.32)	304 (8.6)	1 (620)	2.97	3.01	82	0.865	3.5	8.6	5.1
	820	0.9	1.0	0.994 (5)	−40.1(0.17)	303 (4.4)	1 (320)							
			78.5	0.971 (6)	−38.9(0.17)	305 (4.4)	1 (320)	3.22	3.45	94	0.917	3.5	6.0	5.3
		1.2	1.0	1.001 (5)	−40.8(0.16)	301 (4.4)	1 (320)							
			78.5	0.978 (5)	−39.7(0.17)	301 (4.4)	1 (320)	3.01	3.11	86	0.880	3.7	7.9	5.5
TIP4P	216	0.9	1.0	0.991(10)	−41.2(0.35)	302 (8.7)	1 (630)							
			78.5	0.987(11)	−40.7(0.34)	303 (8.7)	1 (640)	2.25	1.95	47	0.888	3.1	5.0	4.0
	820	0.9	1.0	0.994 (5)	−41.2(0.19)	302 (4.5)	1 (330)							
			78.5	0.989 (6)	−40.9(0.19)	303 (4.5)	1 (330)	2.12	1.83	44	0.861	3.2	6.6	4.3
		1.2	1.0	0.999 (5)	−41.4(0.18)	301 (4.5)	1 (330)							
			78.5	0.992 (5)	−41.1(0.18)	301 (4.4)	1 (320)	2.43	2.17	52	0.929	3.5	3.8	4.6
SPC/RF	216	0.9	78.5	0.998(11)	−41.7(0.33)	303 (8.7)	0 (650)	2.40	2.18	57	0.887	3.1	5.8	4.1
	820	0.9	78.5	0.999 (6)	−41.6(0.17)	304 (4.5)	1 (330)	2.57	2.40	62	0.891	3.9	5.9	5.2
		1.2	78.5	1.001 (6)	−42.2(0.17)	301 (4.4)	1 (330)	2.54	2.36	62	0.923	3.4	4.4	4.6
TIP4P/RF	216	0.9	78.5	1.003(11)	−42.0(0.35)	302 (8.7)	1 (650)	2.31	2.05	51	0.862	4.0	6.3	5.2
	820	0.9	78.5	1.002 (6)	−42.2(0.19)	303 (4.5)	1 (330)	2.06	1.76	43	0.867	3.3	5.5	4.2
		1.2	78.5	1.003 (6)	−42.4(0.18)	301 (4.5)	4 (330)	2.22	1.93	48	0.938	3.2	3.2	4.2
Expt				0.9965	−41.7				2.9	78.5				8.3
Ref.				66	39				40	67				43, 68, 44

[a]SPC/E energies including polarization correction.

Dielectric constants $\varepsilon(0)$ were calculated from the fluctuations in the total dipole moment $\langle \boldsymbol{M}^2 \rangle$ of the system[21] using a Clausius–Mosotti-type equation for reaction fields,

$$\frac{\varepsilon(0)-1}{3}\,\frac{2\varepsilon_{\mathrm{rf}}+1}{2\varepsilon_{\mathrm{rf}}+\varepsilon(0)}=\frac{\langle \boldsymbol{M}^2\rangle}{9\epsilon_0 V k_B T}, \tag{10}$$

where ϵ_0 is the vacuum permittivity, V is the volume, k_B is Boltzmann's constant, and T is the temperature. When a cutoff is applied, the fluctuations of the total dipole moment $\langle \boldsymbol{M}^2 \rangle$ do not converge to a physically meaningful number,[21] therefore we have listed the dielectric properties for the reaction field simulations only. The resulting dielectric constants are given in Table II. A comparison with literature values is given in Sec. IV H. To estimate the uncertainty in $\varepsilon(0)$ we have plotted the convergence of $\varepsilon(0)$ as a function of simulation time (Fig. 1). From the curves in Fig. 1 we have determined the standard deviation, which is largest for TIP3P

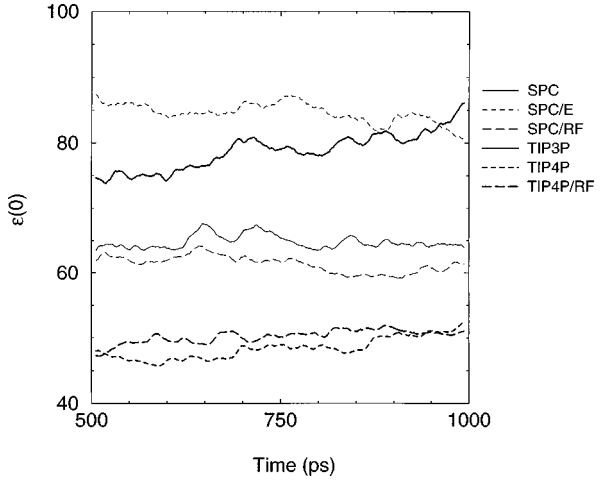

FIG. 1. Convergence of $\varepsilon(0)$ in all simulations with cutoff $r_c=1.2$ nm. A running average over 12.5 ps is shown for clarity.

water (3). However, since there is some drift in most curves we estimate the uncertainty in $\varepsilon(0)$ to be about 5.

The frequency-dependent dielectric constant $\varepsilon(\omega)$ of the system can be determined from the normalized autocorrelation function $\Phi(t)$ of $\boldsymbol{M}$,

$$\Phi(t)=\frac{\langle \boldsymbol{M}(0)\boldsymbol{M}(t)\rangle}{\langle \boldsymbol{M}^2\rangle} \tag{11}$$

using its Fourier–Laplace transform,[41]

$$\frac{\varepsilon(\omega)-1}{\varepsilon(0)-1}\frac{2\varepsilon_{\mathrm{rf}}+\varepsilon(0)}{2\varepsilon_{\mathrm{rf}}+\varepsilon(\omega)}=\int_0^\infty\left(-\frac{\mathrm{d}\Phi}{\mathrm{d}t}\right)e^{-i\omega t}\mathrm{d}t. \tag{12}$$

The autocorrelation function $\Phi(t)$ consists of an initial fast decay to about 90% of the amplitude, followed by a main single exponential decay. With the time resolution that we employed (a sampling rate of 2 per ps was used), no details of the fast decay could be obtained. We therefore modeled the autocorrelation as follows:

$$\Phi(t)=Ae^{(-t/\tau_M)}+(1-A)(1-\theta(t)), \tag{13}$$

where $\theta(t)$ is the Heaviside function ($\theta(t)=0$ for $t<0$ and $\theta(t)=1$ for $t\geqslant 0$). The simulation results were fitted to this equation by a weighted least squares procedure. The statistical weights were the inverse variances of the correlation data points, obtained from a block-averaging procedure (using nine blocks of 100 ps). The range of time values over which the fit was made was taken from 0.5 to 8 ps, but the upper boundary was varied from 7 to 10 ps to assess the reliability and accuracy of the results. The values of τ_m and A are given in Table II; their accuracies are about 0.1 ps and 0.01, respectively.

By solving Eq. (12) for $\varepsilon(\omega)$, using Eq. (13), we find the simple expression,[42–44]

$$\frac{\varepsilon(\omega)-\varepsilon(\infty)}{\varepsilon(0)-\varepsilon(\infty)}=\frac{1}{1+i\omega\tau_D}, \tag{14}$$

where

$$\varepsilon(\infty)=1+\frac{(1-A)(\varepsilon(0)-1)}{1+A\lambda}, \tag{15}$$

and

$$\tau_D=(1+A\lambda)\tau_M. \tag{16}$$

Here $\lambda=(\varepsilon(0)-1)/(2\varepsilon_{\mathrm{rf}}+1)$. Thus we see that a Debye relaxation is found with a high-frequency limit and with a time constant that exceeds the time constant of the collective dipole relaxation by a factor roughly equal to 1.5. For simulations with conducting boundary conditions or, equivalently, using Ewald summation, $\lambda=0$ and the two relaxation times are then equal. The values of τ_D and $\varepsilon(\infty)$ are given in Table II. Comparison with literature values of τ_D is given in Sec. IV H.

Equation (12) can also be used to compute $\varepsilon(\omega)$ directly from $\Phi(t)$. In order to calculate $\mathrm{d}\Phi/\mathrm{d}t$ we combined the first 10 ps of $\Phi(t)$ with the tail obtained from the fit, the curve was extended to 500 ps. To prevent artifacts because of the connection between data and fit we made a smooth transition by linear interpolation over the data points between 5 and 10 ps. Finally, the derivative $\mathrm{d}\Phi/\mathrm{d}t$ was calculated numerically. We have plotted the real part of $\varepsilon(\omega)$ for the 820 molecule simulations with $r_c=1.2$ nm in Fig. 2, together with experimental data from Ref. 43. The high-frequency range of the computed results is not reliable because of the sampling rate used. It is clear from Fig. 2 that $\varepsilon(\omega)$ is well reproduced in the SPC/E simulation over the entire frequency range spanned by the experimental results. Furthermore we see, as expected, that SPC is very similar to SPC/RF while TIP4P is very similar to TIP4P/RF. Since the low frequency part of $\varepsilon(\omega)$ is determined by the fit, and therefore by the Debye relaxation time τ_D it comes as no surprise that the SPC/E model is the best, since the SPC/E model also has the best correspondence with experimental results for τ_D.

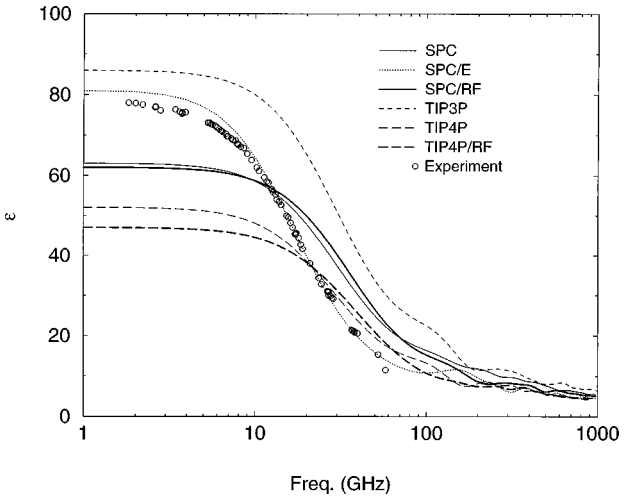

FIG. 2. The frequency dependence of the dielectric constant [$\varepsilon(\nu)$] from the 820 molecule simulations with a 1.2 nm cutoff. Experimental values from Ref. 43 are given for comparison. Please note that $2\pi\nu=\omega$.

We have also studied relaxation processes of the water models, which can be determined experimentally by nuclear magnetic resonance (NMR). The relaxation properties can be characterized by reorientational correlation functions,

$$C_l^\alpha=\langle P_l(\mathbf{e}^\alpha(t)\cdot\mathbf{e}^\alpha(0))\rangle, \tag{17}$$

where P_l is the lth rank Legendre polynomial and $\mathbf{e}^\alpha$ is the unit vector which points along the α axis in the molecular reference frame. For our analyses we have used four different axes; the H–H axis which can be measured by ^{1}H–^{1}H dipolar relaxation NMR experiments, the molecular dipole μ, which can be related to dielectric relaxation of the bulk, the O–H axis which can be measured by ^{17}O–^{1}H dipolar relaxation in NMR experiments. Finally we have computed the rotational correlation time of the normal $\perp$ to the water plane, defined as $\perp=\boldsymbol{r}_{\mathrm{OH1}}\times\boldsymbol{r}_{\mathrm{OH2}}$. The single molecule correlation times τ_l^α can be obtained by integrating the correlation functions[45,46] or fitting the correlation function using the following expression:

$$C_l^\alpha(t)=e^{-t/\tau_l^\alpha}. \tag{18}$$

It is well known that the tails of correlation functions converge slowly.[1] Therefore, we have used a combined method,

TABLE III. Overview of dynamic and structural properties from the reference simulations and the simulations with the new SPC/RF and TIP4P/RF water models, derived from the last 900 ps. Diffusion constant D with standard deviation and rotational correlation time τ and position and height of first and second peak in the oxygen–radial distribution function $g(r)$. The error in the correlation times were estimated to be 0.1 ps by varying the integration procedure (see text).

Model	N	r_c (nm)	ϵ_{rf}	D (10^{-9} m^{12}/s)	τ_1^{HH} (ps)	τ_1^{μ} (ps)	$\tau_1^{\perp}$ (ps)	τ_1^{OH} (ps)	τ_2^{HH} (ps)	τ_2^{μ} (ps)	$\tau_2^{\perp}$ (ps)	τ_2^{OH} (ps)	r_1 (nm)	$g(r_1)$	r_2 (nm)	$g(r_2)$
SPC	216	0.9	1.0	4.1(0.19)	2.4	2.6	1.6	2.5	1.1	0.9	0.7	1.0	0.275	2.85	0.445	1.07
			78.5	4.6(0.09)	2.1	2.2	1.4	2.2	1.0	0.8	0.6	0.9	0.275	2.85	0.465	1.08
	820	0.9	1.0	4.3(0.07)	2.4	2.7	1.7	2.5	1.1	1.0	0.7	1.0	0.275	2.83	0.455	1.06
			78.5	5.0(0.07)	2.2	2.2	1.5	2.2	1.0	0.8	0.7	0.9	0.275	2.81	0.445	1.05
		1.2	1.0	4.2(0.08)	2.4	3.4	1.8	2.7	1.2	1.1	0.8	1.1	0.275	2.82	0.45	1.06
			78.5	4.5(0.08)	2.3	2.4	1.6	2.4	1.1	0.9	0.7	1.0	0.275	2.82	0.455	1.06
SPC/E	216	0.9	1.0	2.5(0.14)	3.8	4.2	2.6	3.9	1.8	1.5	1.1	1.6	0.27	3.00	0.445	1.11
			78.5	2.9(0.08)	3.4	3.3	2.2	3.4	1.6	1.2	1.0	1.4	0.275	3.02	0.445	1.12
	820	0.9	1.0	2.8(0.06)	3.8	4.3	2.6	3.9	1.8	1.5	1.1	1.6	0.27	2.99	0.45	1.10
			78.5	3.3(0.06)	3.4	3.3	2.2	3.4	1.6	1.2	1.0	1.4	0.27	2.98	0.455	1.11
		1.2	1.0	2.7(0.12)	3.9	5.5	2.8	4.4	1.8	1.7	1.2	1.7	0.275	2.98	0.445	1.10
			78.5	2.8(0.02)	3.8	3.8	2.5	3.8	1.7	1.4	1.1	1.6	0.27	3.00	0.445	1.11
TIP3P	216	0.9	1.0	5.2(0.25)	1.5	2.1	1.2	1.7	0.8	0.7	0.6	0.7	0.275	2.70	0.465	1.01
			78.5	6.5(0.11)	1.4	1.7	1.0	1.5	0.7	0.6	0.5	0.7	0.275	2.67	0.46	1.01
	820	0.9	1.0	5.5(0.10)	1.6	2.2	1.2	1.8	0.8	0.8	0.6	0.7	0.275	2.67	0.46	1.00
			78.5	7.0(0.07)	1.4	1.7	1.0	1.5	0.7	0.6	0.5	0.7	0.275	2.67	0.46	1.01
		1.2	1.0	5.4(0.14)	1.6	3.0	1.3	2.0	0.8	0.9	0.6	0.8	0.275	2.67	0.525	1.01
			78.5	6.2(0.08)	1.5	1.9	1.1	1.7	0.7	0.7	0.5	0.7	0.275	2.68	0.465	1.01
TIP4P	216	0.9	1.0	3.4(0.12)	3.0	2.9	2.0	3.0	1.3	1.0	1.7	1.2	0.275	2.96	0.455	1.11
			78.5	4.0(0.15)	2.8	2.4	1.9	2.9	1.2	0.9	1.6	1.1	0.275	2.93	0.45	1.10
	820	0.9	1.0	4.0(0.08)	3.1	3.0	2.1	3.1	1.3	1.0	1.0	1.2	0.275	2.95	0.435	1.10
			78.5	4.2(0.06)	3.0	2.5	1.9	2.8	1.3	0.9	0.8	1.1	0.275	2.94	0.435	1.09
		1.2	1.0	3.7(0.05)	3.2	3.4	2.2	3.4	1.4	1.1	1.0	1.3	0.275	2.94	0.45	1.10
			78.5	3.9(0.11)	3.1	2.7	2.0	2.9	1.3	1.0	0.9	1.2	0.275	2.97	0.44	1.11
SPC/RF	216	0.9	78.5	4.5(0.21)	2.2	2.2	1.4	2.2	1.0	0.8	0.6	1.0	0.275	2.85	0.455	1.07
	820	0.9	78.5	4.8(0.09)	2.2	2.2	1.5	2.2	1.0	0.8	0.7	1.0	0.275	2.80	0.455	1.05
		1.2	78.5	4.3(0.06)	2.4	2.4	1.6	2.4	1.1	0.9	0.7	1.0	0.275	2.84	0.45	1.07
TIP4P/RF	216	0.9	78.5	3.5(0.22)	3.0	2.6	2.0	2.9	1.4	1.0	1.7	1.2	0.275	3.01	0.445	1.12
	820	0.9	78.5	4.0(0.07)	3.1	2.6	2.0	2.9	1.4	1.0	0.9	1.2	0.275	2.98	0.445	1.10
		1.2	78.5	3.4(0.10)	3.3	2.9	2.2	3.2	1.5	1.1	1.0	1.3	0.275	3.00	0.445	1.11
Expt				2.3					2.0			1.95	0.288	3.09	0.45	1.13
Source				69					51			54–57	5,6			

using explicit integration until 5 ps, and fitted the tail of the correlation function (from 5 through 500 ps) to Eq. (18), and obtained the integral for the tail from the fit. We also computed correlation times using a different time of division between explicit integral and fitting (0, 2.5, 7.5, and 10 ps). All these give similar results, within 0.1 ps for the correlation time. Without any fitting the long time behavior of the correlation function influences the resulting correlation time strongly, such that the results are rather erratic. When pure fitting was used (no explicit integration), the correlation times appeared to be too high systematically. Therefore, we concluded that 5 ps is a good point to switch from integration to fitting. The correlation times τ_l^{α} are printed in Table III along with the self-diffusion constant D, and structural properties [position and height of first and second peak in the oxygen–oxygen radial distribution function $g_{OO}(r)$].

Diffusion constants were calculated from the mean square displacement (MSD) using the Einstein relation.[1] To assess the uncertainty in the results, we again used a block averaging procedure over five partially overlapping blocks of 500 ps (100–600 ps, 200–700 ps, etc.). The convergence of diffusion constants can be monitored by plotting $D=$(MSD/6 t) for $t>0$ against time t (data not shown). For short times (<100 ps) fluctuations of $\pm 0.3\times 10^{-5}$ cm^2 s^{-1} around the average could be seen, but we found that the D were sufficiently converged after 300 ps. Therefore we used of the 500 ps MSD plots only the last 200 ps to determine D. The average and standard deviation of the five diffusion constants determined in this manner are given in Table III. A comparison with literature values is given in Sec. IV H.

In the following sections we first describe the effects caused by varying the simulation parameters, system size, cutoff and reaction field. Then we discuss the results for rotational correlation, then the derivation and quality of the new parameter sets for SPC/RF and TIP4P/RF. Finally we discuss structural properties, and give a comparison of our results with literature values from simulations.

A. Effects of system size

If we compare results for small (216 molecules) and large (820 molecules) systems simulated with the same cutoff ($r_c=0.9$), we see that the average thermodynamic properties (ρ, E_{pot}, T, P) are the same. The amplitude of the fluctuations is proportional to the square root of the number of particles, in our case the ratio large : small system should be $\sqrt{820/216}=1.95$, which is indeed what we find for the fluctuations in the thermodynamic properties. It should be noted however, that the magnitude of the fluctuations is reduced systematically when the weak coupling algorithm for temperature and pressure scaling is applied,[47] but the dependence on the number of molecules is correct. The similarity between averages and fluctuations is also found when a reaction field is applied.

A number of differences between large and small systems can be noted. We see that the dielectric constant $\varepsilon(0)$ is higher for all models in the larger system, and we also see that in all models the diffusion constant is higher in the larger system. Most likely, these effects are caused by the periodic boundary conditions (PBC). The long-range dipole–dipole correlation between molecules is broken or distorted by the PBC in the small system, leading to lower shielding of electrostatic interactions. Friction caused by PBC may lead to lower diffusion constants. We should therefore conclude that 216 molecule system is too small to accurately calculate the properties of the water model.

B. Effects of cutoff

We have simulated the 820 molecule system with a cutoff of 0.9 and 1.2 nm. In all models, we see that the density increases on increasing the cutoff. Furthermore, in all models, the energy decreases when the cutoff is increased. Finally, the average temperature drops by 2 or 3 K in all models on increasing the cutoff. There is no clear systematic effect on the dielectric behavior from increasing the cutoff, but in all models the diffusion constant is reduced. To investigate fluid structure beyond the cutoff, we plotted the distance dependent Kirkwood factor $G_k(r)$ (Ref. 8) according to

$$G_k(r)=\sum_{r_{ij}<r}\frac{\boldsymbol{\mu}_i\cdot\boldsymbol{\mu}_j}{\mu^2}, \tag{19}$$

where $\boldsymbol{\mu}_i$ and $\boldsymbol{\mu}_j$ are the dipole vectors of water molecules i and j, respectively, and r_{ij} is the distance between oxygen atoms. In Fig. 3 the $G_k(r)$ are given for all 820-molecule simulations with reaction field and two different cutoffs. There is a large difference between curves of the same model but simulated with different cutoff. If we presume that a more rigorous treatment, i.e., a larger cutoff, leads to more realistic results, we must conclude that a considerable amount of dipole–dipole correlation is lost when a cutoff of 0.9 nm is used. It can however not be ruled out that the ''real'' $G_k(r)$ function is an intermediate between the two. We would like to emphasize that the shape of the curve is highly dependent on the center used for calculating the distance. When the center of geometry is used, a very different curve is obtained, therefore we have used the oxygen atom like is used in most literature studies. Finally, all curves show a slight dip before the cutoff distance. This effect has been attributed by Smith and van Gunsteren to the fact that the simulation employs a reaction field permittivity $\varepsilon_{\mathrm{rf}}$ that differs from the dielectric constant of the water model used.[48]

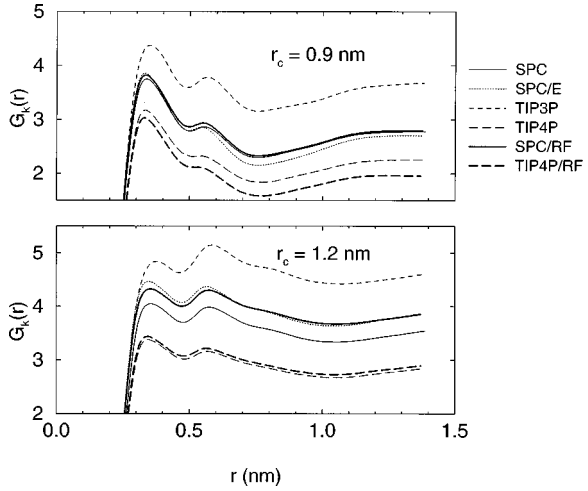

FIG. 3. Distance dependent Kirkwood factor $G_k(r)$ for the 820 molecule boxes of all water models, simulated with reaction-field and cutoff $r_c=0.9$ nm (top), respectively, $r_c=1.2$ nm (bottom).

C. Effects of the reaction field

In all simulations we see that the density is reduced and the energy is increased by about 1 kJ mol^{-1} when a reaction field is applied. We note that the difference between simulation with and without reaction field would be even more serious if we had not applied the long-range correction for dispersion; the energy correction is about -0.25 kJ mol^{-1} ($r_c=0.9$ nm) resp. -0.1 kJ mol^{-1} ($r_c=1.2$ nm), the pressure correction is about -200 bar ($r_c=0.9$ nm), resp. -80 bar ($r_c=1.2$ nm). Furthermore, the self-diffusion constant D increases and the rotational correlation times τ_l^{α} decrease when a reaction field is applied (Table III). Thus, the rotational as well as the translational mobility of the molecules are increased by the reaction field, probably because of two interconnected reasons; the reduced intermolecular forces and the reduced density. The effects of a reaction field on dipole–dipole correlation and consequently on dielectric properties have been discussed in the preceding section, as well as in the literature,[7,10,49] therefore we will not discuss this issue here.

D. Rotational correlation

The rotational correlation of water has been studied for many years, predominantly by NMR techniques.[50–57] A complicating factor in the analysis of relaxation measurements is that the distance r between the nuclei between which relaxation occurs weighs as r^{-6}. An error of 5% in this distance (which is approximately the difference between the OH bond length *in vacuo* and in ice) leads to a difference of 25% in correlation times. To this end, studies aimed at determining the OH bond length in water have been performed.[56] Another

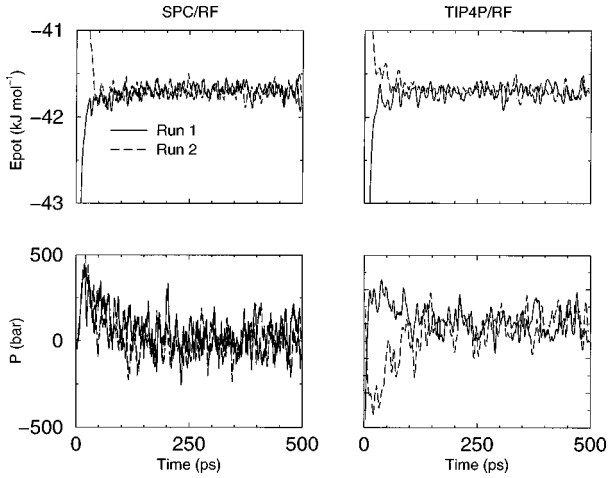

FIG. 4. Convergence of energy to the target value of -41.7 kJ mol^{-1} in SPC/RF (top left) and TIP4P/RF (top right) GCT simulations. Convergence of pressure to the target value of 1 bar in SPC/RF (bottom left) and TIP4P/RF (bottom right) GCT simulations. A running average of the pressure over 5.0 ps (50 data points) was plotted for clarity.

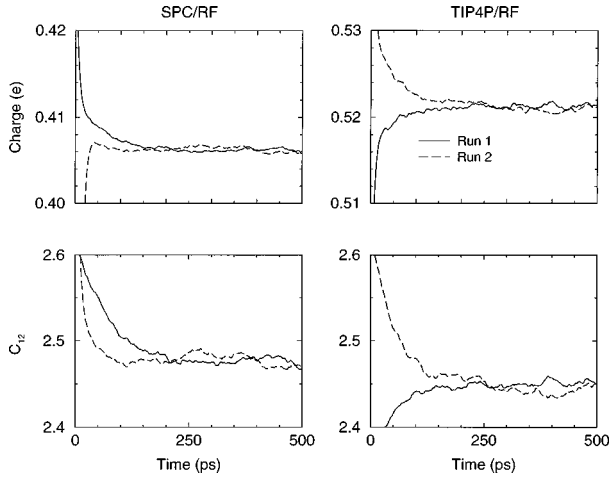

FIG. 5. Convergence of hydrogen charge in SPC/RF (top left) and TIP4P/RF (top right) GCT simulations. The oxygen charge in SPC/RF, respectively, the charge on the dummy particle in TIP4P/RF are simply -2 times the hydrogen charge. Convergence of Lennard-Jones C_{12} (unit 10^{-6} kJ mol^{-1} nm^{12}) in SPC/RF (bottom left) and TIP4P/RF (bottom right) GCT simulations.

complicating factor in the analysis of ^{1}H–^{1}H relaxation is, that inter- and intramolecular contributions can not easily be discriminated. Moreover, it has been argued that the two contributions are of equal magnitude.[52] Nevertheless, the experimental values for the reorientational correlation times have converged to about 2.0 ps (Table III) in the scientific literature. Our MD results for τ_2^{HH} and τ_2^{OH} are all too low, the SPC/E model with 1.2 nm cutoff being closest to the experimental values (Table III).

The question whether water rotation in solution is isotropic has long been a matter of dispute. The experimental data seem to prove that this is indeed the case, but there is, to our knowledge, no experimental source for the rotational correlation of the $\perp$ vector (normal to the water plane). In our simulations $\tau^{\perp}$ is almost always significantly smaller than the correlation times in the plane of the molecule.

The ratio between corresponding τ_1 and τ_2's are an indication for the type of diffusional process. For a rotational diffusion that consists of small angular steps with rotational diffusion constant D, the lth spherical harmonic function decays exponentially with a time constant $\tau_l=[Dl(l+1)]^{-1}$, and thus $\tau_1=3\tau_2$. For rotational diffusion consisting of larger angular jumps the τ_1/τ_2 ratio is expected to be smaller. This is what we observe in the majority of the simulations, the above mentioned ratio is closer to 2 than to 3.

E. Derivation of SPC/RF and TIP4P/RF force field

The convergence of both GCT simulations for SPC/RF and TIP4P/RF can be monitored from the convergence of the actual energy to the target value, and the convergence of the actual pressure to the target value (Fig. 4). Similarly the convergence of the force field, charges and Lennard-Jones C_{12} are plotted in Fig. 5. Judging from both figures, the simulations are converged after 300 ps. We therefore took the force field parameters to be the average over the last 200 ps of both simulations for either SPC/RF and TIP4P/RF giving 4000 data points for each parameter. The resulting parameters are given in Table I. The charges in SPC/RF and TIP4P/RF differ only slightly from the corresponding SPC and TIP4P values. Since the energies of the standard SPC and TIP4P with and without reaction field differ only slightly, this is not surprising. The Lennard-Jones C_{12} parameter for SPC/RF is reduced by a considerable 6%. However, since the density of the standard SPC with (and even without) reaction field is quite low, this is not unexpected either. For TIP4P/RF the C_{12} parameter is reduced only slightly.

We computed the relaxation time for the charge in our GCT simulations, by fitting an exponential function the plots in Fig. 5. We found τ_E to be 10 ps, resp. 19 ps (SPC/RF) and 12 ps resp. 18 ps (TIP4P/RF). Similarly we found τ_P, corresponding to the relaxation of C_{12} by coupling to the pressure, to be 12 ps resp. 69 ps (SPC/RF) and 64 ps resp. 62 ps (TIP4P/RF). Averaged over the four simulations $\tau_E=15$ ps, while $\tau_P=52$ ps. Using Eq. (7) we estimate $\langle \partial E/\partial q_H \rangle$ to be about -81 kJ mol^{-1} e^{-1}. This value is closer to that of Zhu and Wong[35] (-50) than to that reported by Berendsen *et al.*[4] (-260), but this not unexpected, since the latter authors performed relatively short simulations. It should be noted, that the GCT simulation are by definition nonequilibrium simulations (i.e., not with constant force field), therefore our values can not be directly compared to those in the literature.

F. Quality of the SPC/RF and TIP4P/RF models in free simulations

The SPC/RF water model that we have optimized for use with a reaction field, reproduces the correct potential energy in a free simulation (Table II), at least when simulated with $r_c=0.9$ nm. The potential energy for SPC/RF is somewhat lower when a cutoff of 1.2 nm is used. For TIP4P/RF the energy is about 0.5 kJ mol^{-1} lower than the reference energy in the system used for parametrizing (820 molecules, $r_c=0.9$ nm). The density is slightly too high for both SPC/RF and TIP4P/RF. However, for both models the density and potential energy are close to the experimental values. Com-

TABLE IV. Values from the literature for diffusion constant D, dielectric constant $\varepsilon(0)$, and Debye relaxation time τ_D. Where given in the original reference, errors are given within parentheses. We included simulations of the original rigid water models only. Under the heading LR (long-range electrostatics) we use the following abbreviations to distinguish the methods use to treat the long-range electrostatics: SC (spherical cutoff), EW (Ewald), RF (reaction field), SF (switching function).

Model	N	LR	r_c (nm)	ε_{rf}	Time (ps)	ρ (kg/ℓ)	E_{pot} (kJ/mol)	T (K)	P (bar)	D (10^{-9} m^2/s)	$\varepsilon(0)$	τ_D (ps)	Ref.
SPC	216	SC	0.85	1.0	12.5	1	−42.2	300		3.6			2
	216	SC	0.9	1.0	20	0.970	−41.4	300	−0.9	4.3			4
	216	SC	0.85	1.0	50	0.996	−41.8(0.2)	301(5)	700(300)	4.4(0.1)			70
	108	EW			MC[a]	1	−38.6	300			63(31)		71
	265	EW	0.985		1019	0.965		300			67.8(6.7)		25
	216	EW			700	0.997	−41.8	298	300	3.6(0.5)	72(7)	11(2)	58
	216	EW			200	1	−41.1	300	2000	4.5(0.5)			72
	216	EW			40.0	1	−39.5	299		4.69			73
	126	EW	0.775		800	0.992	−40.9(0.1)	300			66.6(2.6)		74
	345	EW	1.085		500	0.993	−40.9(0.1)	300			77.1(10.9)		74
	216	SC	0.93	1.0	120	0.996	−41.3(0.1)	309		4.1(0.2)			45
	1000	SC	1.55	1.0	25.0	0.996	−41.91(0.05)	300		4.2(0.2)			45
	216	EW			144	0.996	−41.1(0.2)	300		4.2(0.2)			45
	216	SF	0.85	1.0	50	1	−41.8	300		4.6(0.2)			75
	512	SC	0.9	1.0	1000	0.980		300	28	3.9			12, 22
	512	RF	0.9	∞	1000	0.953		300	2	5.3	57.3	4.0	12, 48, 22[b]
	216	SC	0.9	1.0	10.0	1		298		4.4(0.1)			76
SPC/E	216	SC	0.9	1.0	27.5	0.998	−46.3[c]	306	6	2.5			4
	216	EW			700	0.997	−46.7	298	0	2.4(0.4)	70(9)		58
	256	EW			200			300		2.6(0.1)	81.3		77
	216	RF	0.92		150	1.0		300		2.43			78
	512	RF	0.9	1.0	1000	1.002	−47.0	300	−5	2.7	53.1	4.9	12, 48, 22[b]
	512	RF	0.9	62.3	1000	0.976		300			62.7	6.0	12, 48, 22[b]
	512	RF	0.9	∞	1000	0.976	−45.9	300	−37	3.2	64.0	5.4	12, 48, 22[b]
	360	SC	0.9	1.0	400	1.0013	−44.28	307.4		2.51(0.22)			79
	216	EW			600	0.997	−46.64	298	−80(40)	2.4(0.4)	67(10)	10(3)	80
	256	EW			500	0.998	−46.72	298		2.24	71.0(7.4)	9.7	46
	216	EW	0.95			0.997	−46.3	300.6		4.4			81
	216	EW			200	0.999		303.15	69(17)	2.75(0.05)			82
	512	EW			200	0.9956		303.15	−7(20)	2.76(0.06)			82
TIP3P		RF	0.8	78.3	10–30		−38.5	300	1		96		7
		EW			20	0.98		300	1	3.98			83
TIP4P	343	EW	1.093		16.2	0.983	−41.2	300	370	4.5			84
	216	SF	0.85			0.999		298	1	2.96			85
	345	SC	1.085		630	0.993	−41.4	293			51.7(10.8)		25
	216	RF	0.8	∞	570	0.999	−41.4	293			25.9(2.7)		25
	216	EW			700	0.997	−41.6	298	0	3.3(0.5)	61(7)	7(2)	58
	216	RF	0.985	∞	2000	1.0	−41.5	293		2.8	53		86

[a]Monte Carlo.
[b]See text.
[c]SPC/E energies including polarization correction.

pared to their respective original models, both SPC/RF and TIP4P/RF have better density and potential energy, which proves that the parameterization method works. Of course this is no guarantee for better overall properties. If we compare SPC/RF to SPC with a reaction field, we see that the diffusion constant D is slightly better in SPC/RF, but the dielectric constant is slightly lower. The dynamic properties of the TIP4P/RF model are significantly better than those of the TIP4P model with a reaction field.

G. Comparison of structural properties

Structural properties, in particular the oxygen–oxygen radial distribution function (RDF) have always played an important role in assessing the quality of water models. The most important features of the O–O RDF, the location and height of the first and second peak have been tabulated (Table II). In all models the position of the first peak is at 0.275 nm, but the height varies from 2.67 (TIP3P) to 3.02 (SPC/E). The second peak is located around 0.45 nm, and the height varies from 1.0 (no peak, TIP3P) to 1.12 (TIP4P/RF). We should however be careful in interpreting these results, because some systematic effects can be observed. In all models, the height of both peaks is slightly larger in the 216 molecules simulation than in the 820 molecule simulation. Furthermore, the use of a reaction field reduces the height of the first peak in the simulations with a cutoff of 0.9 nm, while it increases the height of the first peak in the simulation with 1.2 nm. There is no significant structural difference

between SPC water simulated with a reaction field, and the new SPC/RF model; the new TIP4P/RF model seems to be slightly more structured than TIP4P. The experimental values that we have compared the simulation data to, are from neutron diffraction experiments of Soper and Phillips from 1986.[5] This has been *the* source for structural information of liquid water, and the experimental O–O RDF has even been used for refinement of water models.[58] It should be noted, that in a new analysis of old data and new data from additional experiments by Soper *et al.*, the RDFs were re-evaluated, and the height of the first peak in the O–O RDF has decreased slightly.[6]

H. Comparison with literature

A lot of properties of the water models we have presented here have been calculated previously by other authors. An overview of values for the diffusion constant D, the dielectric constant $\varepsilon(0)$ and the Debye relaxation time τ_D is given in Table IV. We have selected values from the literature that were computed at around 300 K. The diffusion constants we have computed for SPC and SPC/E fall well into the range defined by the literature, both with and without reaction field. For TIP4P our values are slightly higher than those reported in the literature, this is most likely due to system size (see Sec. IV A). For 216 molecules we find $D=3.4\times10^{-9}$ m^2/s which is comparable to previously reported values. All the dielectric constants $\varepsilon(0)$, fall within the range determined by previous studies. Smith and van Gunsteren[48] reported similar τ_M values as in this work. However these authors calculated τ_D from an incorrect equation. When Eq. (16) is applied on their results for the SPC/E water model, values are obtained that are in good agreement with our simulations, and also with experimental data.

Finally we would like to note that the spread in literature results and simulation conditions makes it impossible to draw conclusions on the influence of simulation methodology on the results. In our opinion, this justifies doing all the simulations we have presented in this work.

V. CONCLUSION

Is there predictive value in water computer simulations? This question was raised by Brodsky in a recent review of water simulations,[59] and answered with a clear no. We agree with this answer to some extent, but would like to emphasize that simulations, when performed and analyzed carefully, may still yield useful information. In previous work, we performed simulations of short peptides from BPTI using different water models (SPC, TIP3P, and SPC/E) and peptide force fields.[60] Only one force field/water model combination gave results in agreement with experimental chemical shift data, but using this particular combination we could gain insight in the dynamics of the peptides at a level of detail that is not accessible experimentally.

In this work we have reassessed density and energy, dynamic, dielectric, and structural properties for some of the most popular water models. Our results do not differ significantly from literature values, but by performing all simulations and analyses in exactly the same way, we were able to study the impact of simulation methodology on the results, independent of the water model. We did indeed find that system size, cutoff length, and the use of a reaction field have comparable impact on the results for all water models.

How far are we from the ''ultimate water model'' for classical simulations? Moreover, is there ever going to be such a model? It is obvious that such questions must be raised in the context of the pessimistic view of Brodsky.[59] For nonpolarizable models the model that gives closest agreement with experimental data for bulk water is the SPC/E model.[4] Its built-in polarization energy correction, leading to the enhanced dipole as compared to other models (see Table I), gives a significant improvement in many properties. When combined with a reaction field and a long cutoff we find excellent agreement with experimental data for many important properties (see Tables II and III). It seems that the SPC/E model is close to the ultimate nonpolarizable water model for bulk studies. We would like to add that SPC/E also outperforms many (simple) polarizable models for studies of bulk water (for a review see Zhu *et al.*[61]).

However, water models are most often used in studies of solvated compounds, such as proteins and (biological) membranes. There, the SPC/E model has been found to give dubious results.[62,63] The reason is that SPC/E requires an environment dependent polarization correction which is not applied in simulations. Based on our experience[62–64] we prefer the SPC model for simulations of a solute in water. It should be noted that the TIP3P model, which has almost the same dipole as SPC/E does not perform so well overall. Obviously, the Lennard-Jones parameters and the geometry of the model are important factors as well.

Finally, we conclude from our work that the use of a reaction field does improve the results obtained from simulation. We can also conclude that experimental density and potential energy are reproduced better using the special purpose SPC/RF and TIP4P/RF models than by the corresponding SPC and TIP4P models. However, the properties of the SPC/RF model, optimized for use with a reaction field, are still dependent on the cutoff, and therefore the new SPC/RF and TIP4P/RF should only be used with a cutoff of 0.9 nm. We realize that it is not likely to expect that these two water models will gain great popularity. However, when one wants to employ a reaction field to simulate a solute molecule, such as a peptide (e.g., Ref. 65), the use of either of these models is to be preferred over their respective ancestors.

[1] M. P. Allen and D. J. Tildesley, *Computer Simulations of Liquids* (Oxford Science, Oxford, 1987).
[2] H. J. C. Berendsen, J. P. M. Postma, W. F. van Gunsteren, and J. Hermans, in *Intermolecular Forces*, edited by B. Pullman (Reidel, Dordrecht, 1981), pp. 331–342.
[3] W. L. Jorgensen, J. Chandrasekhar, J. D. Madura, R. W. Impey, and M. L. Klein, J. Chem. Phys. **79**, 926 (1983).
[4] H. J. C. Berendsen, J. R. Grigera, and T. P. Straatsma, J. Phys. Chem. **91**, 6269 (1987).
[5] A. K. Soper and M. G. Phillips, Chem. Phys. **107**, 47 (1986).
[6] A. K. Soper, F. Bruni, and M. A. Ricci, J. Chem. Phys. **106**, 247 (1997).
[7] C. Chipot, C. Milot, B. Maigret, and P. A. Kollman, J. Chem. Phys. **101**, 7953 (1994).
[8] M. Neumann and O. Steinhauser, Mol. Phys. **39**, 437 (1980).
[9] D. J. Adams, E. M. Adams, and G. J. Hills, Mol. Phys. **38**, 387 (1979).
[10] P. Auffinger and D. L. Beveridge, Chem. Phys. Lett. **234**, 413 (1995).

[11] D. van der Spoel, K. A. Feenstra, M. A. Hemminga, and H. J. C. Berendsen, Biophys. J. **71**, 2920 (1996).
[12] P. E. Smith and W. F. van Gunsteren, in *Computer Simulation of Biomolecular Systems*, edited by W. F. van Gunsteren, P. K. Weiner, and A. J. Wilkinson (Escom, Leiden, 1993), Vol. 2, pp. 182–213.
[13] P. P. Ewald, Ann. Phys. (Leipzig) **64**, 253 (1921).
[14] R. W. Hockney and J. W. Eastwood, *Computer Simulation Using Particles* (McGraw–Hill, New York, 1981).
[15] B. A. Luty, M. E. Davies, I. G. Tironi, and W. F. van Gunsteren, Mol. Simul. **14**, 11 (1994).
[16] T. Darden, D. York, and L. Pedersen, J. Chem. Phys. **98**, 10089 (1993).
[17] H. G. Petersen, J. Chem. Phys. **103**, 3668 (1995).
[18] L. Greengard and V. Rokhlin, J. Comput. Phys. **73**, 325 (1987).
[19] R. O. Watts, Mol. Phys. **28**, 1069 (1974).
[20] W. F. van Gunsteren, H. J. C. Berendsen, and J. A. C. Rullmann, Discuss. Faraday Soc. **66**, 58 (1978).
[21] M. Neumann, Mol. Phys. **50**, 841 (1983).
[22] P. E. Smith and W. F. van Gunsteren, Mol. Simul. **15**, 233 (1995).
[23] L. Wang and J. Hermans, J. Phys. Chem. **99**, 12001 (1995).
[24] I. G. Tironi, R. Sperb, P. E. Smith, and W. F. van Gunsteren, J. Chem. Phys. **102**, 5451 (1995).
[25] H. E. Alper and R. M. Levy, J. Chem. Phys. **91**, 1242 (1989).
[26] M. Neumann, J. Chem. Phys. **82**, 5663 (1985).
[27] J. E. Roberts and J. Schnitker, J. Phys. Chem. **99**, 1322 (1995).
[28] J. W. Chung, Master's thesis, University of Groningen, 1993.
[29] S. L. Njo, W. F. Gunsteren, and F. Müller-Plathe, J. Chem. Phys. **102**, 6199 (1995).
[30] C. D. Berweger, W. F. van Gunsteren, and F. Müller-Plathe, Chem. Phys. Lett. **232**, 429 (1995).
[31] A. A. Chialvo and P. T. Cummings, J. Chem. Phys. **105**, 8274 (1996).
[32] H. J. C. Berendsen, D. van der Spoel, and R. van Drunen, Comput. Phys. Commun. **91**, 43 (1995).
[33] D. van der Spoel, A. R. van Buuren, E. Apol, P. J. Meulenhoff, D. P. Tieleman, A. L. T. M. Sijbers, R. van Drunen, and H. J. C. Berendsen, GROMACS *User Manual version 1.5* (Nijenborgh 4, 9747 AG Groningen, The Netherlands), Internet: http://rugmd0.chem.rug.nl/~gmx, 1997.
[34] H. J. C. Berendsen, J. P. M. Postma, A. DiNola, and J. R. Haak, J. Chem. Phys. **81**, 3684 (1984).
[35] S. B. Zhu and C. F. Wong, J. Chem. Phys. **98**, 8892 (1993).
[36] S. B. Zhu and C. F. Wong, J. Chem. Phys. **99**, 9047 (1993).
[37] S. Miyamoto and P. A. Kollman, J. Comput. Chem. **13**, 952 (1992).
[38] R. R. Gabdoulline and C. Zheng, J. Comput. Chem. **16**, 1428 (1996).
[39] J. P. M. Postma, Ph.D. thesis, University of Groningen, 1985.
[40] M. Neumann, Mol. Phys. **57**, 97 (1986).
[41] M. Neumann, O. Steinhauser, and G. S. Pawley, Mol. Phys. **52**, 97 (1984).
[42] P. Debye, *Polar Molecules* (Chemical Catalog, New York, 1929).
[43] U. Kaatze, J. Chem. Eng. Data **34**, 371 (1989).
[44] J. T. Kindt and C. A. Schmuttenmaer, J. Phys. Chem. **100**, 10373 (1996).
[45] A. Wallqvist and O. Teleman, Mol. Phys. **74**, 515 (1991).
[46] I. M. Svishchev and P. G. Kusalik, J. Phys. Chem. **98**, 728 (1994).
[47] E. Paci and M. Marchi, J. Phys. Chem. **100**, 4314 (1996).
[48] P. E. Smith and W. F. van Gunsteren, J. Chem. Phys. **100**, 3169 (1994).
[49] P. E. Smith, R. C. van Schaik, T. Szyperski, K. Wüthrich, and W. F. van Gunsteren, J. Mol. Biol. **246**, 356 (1995).
[50] J. Jonas, T. DeFries, and D. J. Wilbur, J. Chem. Phys. **65**, 582 (1976).
[51] B. Halle and H. Wennerström, J. Chem. Phys. **75**, 1928 (1981).
[52] D. Lankhorst, J. Schreiver, and J. C. Leyte, Ber. Bunsenges. Phys. Chem. **86**, 215 (1982).
[53] J. Teixeira, M. Bellissent-Funel, S. H. Chen, and A. J. Dianoux, Phys. Rev. A **31**, 1913 (1985).
[54] J. R. C. van der Maarel, D. Lankhorst, J. de Bleijser, and J. C. Leyte, Chem. Phys. Lett. **122**, 541 (1985).
[55] R. P. W. J. Struis, J. de Bleijser, and J. C. Leyte, J. Phys. Chem. **91**, 1639 (1987).
[56] T. W. N. Bieze, J. R. C. van der Maarel, and J. C. Leyte, Chem. Phys. Lett. **216**, 56 (1993).
[57] R. Ludwig, Chem. Phys. **195**, 329 (1995).
[58] K. Watanabe and M. L. Klein, Chem. Phys. **131**, 157 (1989).
[59] A. Brodsky, Chem. Phys. Lett. **261**, 563 (1996).
[60] D. van der Spoel, A. R. van Buuren, D. P. Tieleman, and H. J. C. Berendsen, J. Biomol. NMR **8**, 229 (1996).
[61] S.-B. Zhu, S. Singh, and G. W. Robinson, Adv. Chem. Phys. **85**, 627 (1994).
[62] A. R. van Buuren, S. J. Marrink, and H. J. C. Berendsen, J. Phys. Chem. **97**, 9206 (1993).
[63] D. P. Tieleman and H. J. C. Berendsen, J. Chem. Phys. **105**, 4871 (1996).
[64] D. van der Spoel and H. J. C. Berendsen, Biophys. J. **72**, 2032 (1997).
[65] O. Steinhauser and H. Schreiber, J. Mol. Biol. **228**, 909 (1992).
[66] E. Schmidt, *Properties of Water and Steam in SI-Units* (Springer, Berlin, 1969).
[67] R. C. Weast, *Handbook of Chemistry and Physics* (Chemical Rubber, Cleveland, 1977).
[68] J. Barthel, K. Bachhuber, R. Buchner, and H. Hetzenauer, Chem. Phys. Lett. **165**, 369 (1990).
[69] K. Krynicki, C. D. Green, and D. W. Sawyer, Discuss. Faraday Soc. **66**, 199 (1978).
[70] O. Teleman, B. Jönsson, and Engström, Mol. Phys. **60**, 193 (1987).
[71] H. J. Strauch and P. T. Cummings, Mol. Simul. **2**, 89 (1989).
[72] J.-L. Barrat and I. R. McDonald, Mol. Phys. **70**, 535 (1990).
[73] M. Provost, D. van Belle, G. Lippens, and S. Wodak, Mol. Phys. **71**, 587 (1990).
[74] M. Belhadj, H. E. Alper, and R. M. Levy, Chem. Phys. Lett. **179**, 13 (1991).
[75] D. van Belle, M. Froeyen, G. Lippenns, and S. J. Wodak, Mol. Phys. **77**, 239 (1992).
[76] D. N. Bernardo, Y. Ding, K. Krogh-Jespersen, and R. M. Levy, J. Phys. Chem. **98**, 4180 (1994).
[77] Y. Guissani and B. J. Guillot, J. Chem. Phys. **98**, 8221 (1993).
[78] I. I. Vaisman, L. Perera, and M. L. Berkowitz, J. Chem. Phys. **98**, 9859 (1993).
[79] L. A. Báez and P. Clancy, J. Chem. Phys. **101**, 9837 (1994).
[80] D. E. Smith and L. X. Dang, J. Chem. Phys. **100**, 3757 (1994).
[81] D. M. Heyes, J. Chem. Soc., Faraday Trans. **90**, 3039 (1994).
[82] S. Balasubramanian, C. J. Mundy, and M. L. Klein, J. Chem. Phys. **105**, 11190 (1996).
[83] E. S. Boek, P. V. Coveney, S. J. Williams, and A. S. Bains, Mol. Simul. **18**, 145 (1996).
[84] M. Ferrario and A. Tani, Chem. Phys. Lett. **121**, 182 (1985).
[85] M. R. Reddy and M. Berkowitz, J. Chem. Phys. **87**, 6682 (1987).
[86] M. Neumann, J. Chem. Phys. **85**, 1567 (1986).